Pergamon

Int. J. Heat Mass Transfer. Vol. 39, No. 1, pp. 39–48, 1996
Copyright © 1995 Elsevier Science Ltd
Printed in Great Britain. All rights reserved
0017-9310/96 $9.50+0.00

0017-9310(95)00103-6

Analysis of flow instabilities and their role on critical heat flux for two-phase downflow and low pressure systems

S. NAIR, S. LELE, M. ISHII† and S. T. REVANKAR

School of Nuclear Engineering, Purdue University, West Lafayette, IN 47907, U.S.A.

(*Received* 13 *December* 1993 *and in final form* 27 *February* 1995)

Abstract—A stability analysis of a flow boiling two-phase low pressure and downflow system relative to the occurrence of critical heat flux has been carried out. The problem formulation is based on a time and area averaged one-dimensional drift flux model, with the necessary constitutive equations. A characteristic equation is obtained to predict the onset of flow excursion and density wave oscillations. By non-dimensionalizing the characteristic equation, important groups governing the system stability are determined. The results of the analysis are useful in determining the region of stable operation for downflow in the Westinghouse Savannah River Site Reactor and in avoiding the onset of flow excursions and density wave oscillations. The analytical results for flow excursion are compared with the Babcock and Wilcox flow excursion experimental data with a Savannah River Mark 22 fuel assembly mockup.

1. INTRODUCTION

In two-phase flow systems a number of thermal hydraulic instabilities have been observed. These instabilities are not desirable as they degrade system control and performance, erode thermal margins and lead to mechanical damage. To avoid that, the design philosophy in chemical process, aerospace and power industries is to design the system for stable operation. This requires the knowledge of stability limits for the system of interest.

Unlike the conventional upflow in most commercial nuclear reactors, some research reactors and the heavy water isotope production reactors, such as the Westinghouse Savannah River Site Reactor, have the coolant flowing downwards. This environment is more susceptible to the onset of instabilities in the form of density wave oscillations, flow excursion, flooding and flow reversal, etc. during the pump coastdown or loss of flow accidents. This affects the reactor adversely, increasing the possibility of premature burnout, which will worsen the accident scenario. This makes it all the more essential to develop a predictive method for these instabilities and to know the stability margins for these reactors.

For a low flow, low pressure condition (typical of an accident leading to pump coastdown and reactor depressurization), the study of flow instabilities becomes very important, because of their potential triggering effect leading to the critical heat flux phenomena. There are four instabilities that become important at low flow and low pressure, namely flow excursion, density wave oscillations [1–12], churn-turbulent to annular flow regime transition, and flooding [7]. Flooding is a special case which will occur only in the case of a bottom blockage in a reactor fuel assembly; but any one of the other three instabilities can lead to a hydrodynamically induced CHF. Correlations are available to predict the churn-turbulent to annular flow regime transition and the flooding phenomena, but analysis of steady state and transient conservation equations is necessary to predict the flow excursion and the density wave oscillations.

Excursive instabilities were first analyzed successfully by Ledinegg [13]. Under certain conditions, the curve of steady state system pressure drop vs flow has a negative slope. Since the flow rate is not a single valued function of the pressure drop, a flow excursion may occur. The excursive stability criterion can be obtained from the steady state pump characteristic $\Delta p_{ext} = f_1(\bar{v}_{fi})$ and the internal pressure drop characteristics $\Delta p_{int} = f_2(\bar{v}_{fi})$. The difference between the external and the internal pressure drop results in a transition. For a stable transition,

$$\frac{\partial \Delta p_{ext}}{\partial \bar{v}_{fi}} < \frac{\partial \Delta p_{int}}{\partial \bar{v}_{fi}}. \quad (1)$$

The physical mechanism associated with density wave oscillations is fairly well understood. Basically, density wave oscillations are caused by the lag introduced in the system by the finite speed of propagation of density perturbations. Consider a boiling channel with a subcooled inlet subjected to a constant, parallel channel type pressure drop boundary condition. A perturbation in the inlet velocity will create a propagating enthalpy perturbation in the single-phase region. The point at which boiling begins will then be perturbed by the arrival of this enthalpy wave. This

† Author to whom correspondence should be addressed.

NOMENCLATURE

a	amplitude of oscillation
A	cross-sectional area
c_k	kinematic wave velocity
Cr^*	ratio of c_k at $z = \lambda$ and l
C_0	distribution parameter
D	hydraulic diameter
f	friction factor
Fr	Froude number, $\bar{v}_{fi}^2/gl$
g	acceleration due to gravity
i	enthalpy
j	volumetric flux
k	loss coefficient
l	length
N_{pch}	phase change number, $\Omega l/\bar{v}_{fi}$
N_d	drift number, $v_{fi}^* + (z^* - \lambda^*) + v_{gj}$
N_ρ	density number (ratio), ρ_g/ρ_f
N_{sub}	subcooling number, $\Delta i_{sub}/\Delta i_{fg}\Delta\rho/\rho_g$
N_G	geometry number
P_{system}	system pressure
Δp	pressure drop
$Q(s)$	characteristic transfer function
q_0''	wall heat flux
Re	Reynolds number based on the inlet velocity, $\rho_f \bar{v}_{fi} D/\mu_f$
s	perturbation parameter
v	velocity
v_{gj}	drift velocity
v_{gj}	local slip velocity
x	quality.

Greek symbols

α	void fraction
Γ_k	Mass generation for k phase
δ	fluctuating component
ε	surface roughness
λ	location of the boiling boundary
ξ	heated perimeter
ρ	density
$\Delta\rho$	density difference between the phases
σ	surface tension
τ	resident time
ω	frequency of oscillation
Ω	reaction frequency.

Subscripts

e	exit
f	liquid
fi	at the inlet to the heated section
fs	saturated liqid
g	vapor
gs	saturated vapor
i	inlet
m	mixture
me	mixture in the unheated exit section.

Superscripts

*	dimensionless quantity
—	steady or average value.

will result in a propagating void fraction perturbation, and thus a density wave in the two-phase region.

Due to the change in flow rate and non-boiling length, there will be a perturbation in the two-phase pressure drop. Since the pressure drop across the channel is imposed externally, there will be a feedback perturbation in the single phase pressure drop. Because of the lags associated with the finite speed of propagation of the enthalpy and void fraction perturbations, the resultant pressure drop perturbation in the two-phase region and the corresponding feedback perturbation in the single-phase region will normally be out of phase with the inlet velocity perturbation. Depending on the lag, the resultant pressure drop perturbation in the single-phase region may either reinforce or attenuate the subsequent inlet velocity perturbation.

Flooding and churn-turbulent to annular flow regime transition are two important static instabilities that can result in the occurrence of critical heat flux at low flow and low pressure conditions. Hence, it is important to predict these instabilities for given operating conditions. Critical heat flux due to flooding occurs when the bottom of the subassembly is blocked. The net flow through the system is zero because the vapor prevents any downward flow of the liquid. Critical heat flux due to the flow regime transition from churn-turbulent to annular flow occurs due to the dryout of the liquid film which cannot be wetted by the liquid slug. Correlations are given for the flooding and churn-turbulent to annular flow regime transition in terms of the heat flux, and these static instabilities can be predicted using the correlations. It is important to perform an analysis of the steady state and transient conservation equations to predict flow excursions and density wave oscillations.

2. PROBLEM FORMULATION

The system shown in Fig. 1(a) is used to understand the mechanism of thermally induced flow instabilities. It is a schematic representation of the real physical system, The Westinghouse Savannah River Site Reactor channel. Here the mathematical model is formulated and the assumptions used to solve the problem are given. The system consists of a channel having flow with heat addition between two volume capacitances. In the real system the volume capacitances are the riser and the downcomer which can insulate any systematic propagation of disturbances. The system under consideration does not include the riser and

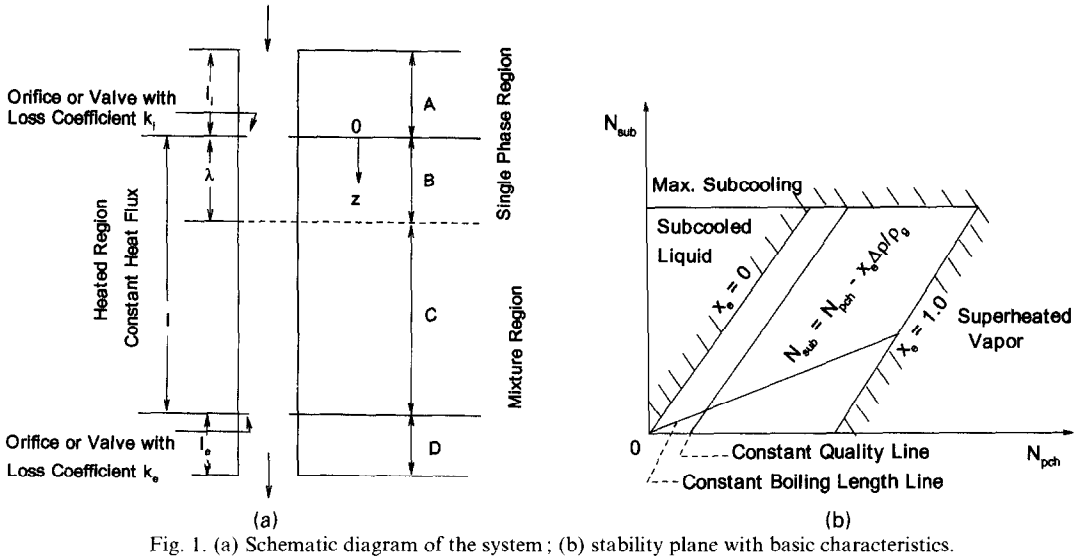

Fig. 1. (a) Schematic diagram of the system; (b) stability plane with basic characteristics.

the downcomer, or components like the pump and turbine.

The system is subdivided into four regions, namely the upstream unheated region, denoted by [A], the heated liquid region, denoted by [B], the heated mixture region, denoted by [C], and the downstream unheated region, denoted by [D]. The thermodynamic process begins with the subcooled liquid of enthalpy i_1, entering the heated duct [region B], with velocity v_{fi}. The heat flux imposed on region [B] is assumed to be constant. In the case of an accident, when the reactor is shut down, the heat flux decreases rapidly during the beginning of the transient, but once it drops down to about 8–10% of full power, it decreases very slowly, and hence can be assumed to be a constant for practical purposes.

2.1. *Region A*

In this region, the flow is assumed to be incompressible. The process is isenthalpic as this region is unheated. Thus $\rho_f = \rho_f(P_{system}) =$ constant and the continuity equation is given as

$$v_{f0} = \frac{A_c}{A_0} v_{fi}(t) \tag{2}$$

where A_c is the flow area for the heated section and A_0 is the flow area for region [A].

The momentum equation is given by

$$-\frac{\partial p}{\partial z} = \rho_f\left(\frac{\partial v_{f0}}{\partial t} + v_{f0}\frac{\partial v_{f0}}{\partial z} + g_0 + \frac{f_0}{2D_0}v_{f0}^2\right). \tag{3}$$

The friction factor is given as $f_0 = f_0(P_{system}, v_{f0}, \mu_f, \varepsilon_0, D_0)$. For an orifice or a valve at the entrance of region [B], $\Delta p_i = k_i \rho_f v_{fi}^2$.

2.2. *Region B*

For this region the following assumptions are made. The pressure and dissipative effects on the liquid enthalpy are neglected. There is thermal equilibrium between phases. The heat source generates steady heat flux. The wall heat capacity is neglected in comparison with fluid heat capacity. Axial heat conduction and normal stresses are neglected. Standard one-dimensional single-phase flow formulation is used here. The equation of state is $\rho_f = \rho_f(P_{system}) =$ constant.

2.3. *Region C*

In this region the thermodynamic processes are assumed to take place at constant pressure, so that $\rho = \rho(i)$ only. Pressure and dissipation effects on mixture enthalpy are neglected. The surface effects are neglected. A one-dimensional time and area averaged drift flux model is used [3].

The mixture continuity equation is given by

$$\frac{\partial \rho_m}{\partial t} + \frac{\partial \rho_m v_m}{\partial z} = 0. \tag{4}$$

The mixture energy equation is given by

$$\rho_m\left(\frac{\partial i_f}{\partial t} + v_m\frac{\partial i_m}{\partial z}\right) = \frac{q_0''\xi}{A_c} - \frac{\partial}{\partial z}\left(\frac{\alpha\rho_g\rho_f}{\rho_m}\bar{v}_{gj}\Delta i_{fg}\right) \tag{5}$$

and the mixture momentum equation is given by

$$-\frac{\partial p}{\partial z} = \rho_m\left(\frac{\partial v_m}{\partial t} + v_m\frac{\partial v_m}{\partial z} + g + \frac{f_m}{2D}v_m^2\right) + \frac{\partial}{\partial z}\left(\frac{\rho_f - \rho_m}{\rho_m - \rho_g}\frac{\rho_g\rho_f}{\rho_m}\bar{v}_{gj}^2\right). \tag{6}$$

Standard equations of state and constitutive relations for drift velocity, mixture friction factor and imposed heat flux are used.

2.4. *Region D*

In this region the process is isenthalpic and the pressure effects on the mixture properties are neglected. The formulation is similar to that of region [C]. For

an orifice or valve at the exit of region [C], $\Delta p = k_e \rho_m(l,t) v_m^2(l,t)$.

3. METHOD OF SOLUTION

The objectives are to obtain the transient response of the system and to determine the stability criteria for the system. The origin of the axial coordinate is chosen to be the boundary between regions [A] and [B], i.e. $z = 0$ at the boundary of [A] and [B]. The initial and the boundary conditions are: at $z = 0$, $t \geqslant 0$,

$$i_f = i_1 = \text{constant} \quad v_f = v_{fi}(t) = \bar{v}_{fi} + \delta v(t).$$

The velocity perturbation is modeled using frequency response: $\delta v(t) = \varepsilon e^{st}$, where s is the perturbation parameter defined as $s = a + jw$. Along with the response of pressure perturbation, use the heat flux boundary condition q_0'' and rheological constitutive relation for friction factor f_m to obtain the characteristic equation: $\delta(\Delta p) = Q(s)\delta(v)$ or $\delta(v) = \delta(\Delta p)/Q(s)$. The asymptotic stability of the system is determined by the nature of roots of the characteristic equation $Q(s) = 0$.

The boiling boundary is obtained from the energy equation in region [B] and can be expressed as:

$$\lambda(t) = \bar{\lambda} + \delta\lambda = \bar{v}_{fi}\tau_{12} + \frac{\varepsilon e^{st}}{s}[1 - e^{s\tau_{12}}]. \tag{7}$$

In the heated mixture region [C], assuming the condition of constant properties for the liquid and vapor phases, and using a correlation for the vapor, drift velocity is given as:

$$\bar{v}_{gj} = f(j,\alpha) = (C_0 - 1)j + v_{gj}. \tag{8}$$

Under these conditions, the mixture and the vapor continuity equations can be transformed into the volumetric flux equation and the density propagation equation as

$$\frac{\partial j}{\partial z} = \frac{\Gamma_g \Delta\rho}{\rho_g \rho_f} \tag{9}$$

which is the volumetric flux equation. Defining the kinematic wave velocity c_k as

$$c_k = j + \bar{v}_{gj} + \alpha \frac{\partial v_{gj}}{\partial \alpha} \tag{10}$$

the density propagation equation is given as

$$\frac{\partial \rho_m}{\partial t} + c_k \frac{\partial \rho_m}{\partial z} = \frac{-\Gamma_g C_0 \rho_m \Delta\rho}{\rho_g \rho_f} + \frac{\Gamma_g (C_0 - 1)\Delta\rho}{\rho_g}. \tag{11}$$

On the other hand, the thermal equilibrium condition gives the relation between vapor generation Γ_g, the heat input and the latent heat:

$$\Gamma_g = \frac{q_0'' \xi}{A_c \Delta i_{fg}}. \tag{12}$$

Define a characteristic frequency of phase change as

$$\Omega = \frac{q_0'' \xi \Delta\rho}{A_c \Delta i_{fg} \rho_g \rho_f} = \frac{\Gamma_g \Delta\rho}{\rho_g \rho_f}. \tag{13}$$

Then the solution for the total volumetric flux is given by

$$j(z,t) = v_{fi}(t) + \Omega(z - \lambda(t)). \tag{14}$$

Assuming the fluctuations in v_{gj} and $\alpha \partial v_{gj}/\partial\alpha$ to be negligible compared with the fluctuations in j, the kinematic wave velocity can be written as

$$c_k(z,t) = \bar{c}_k(z) + \delta c_k(t) = C_0[\bar{v}_{fi} + \Omega(z - \bar{\lambda})] + v_{gj} + C_0 \varepsilon e^{st} \Lambda_1(s) \tag{15}$$

where $\Lambda_1(s)$ is a transfer function between δv and δc_k. The solution for mixture density gives

$$\delta\rho_m(z,t) = \rho_f \varepsilon e^{st} \Lambda_2(z,s) \tag{16}$$

and that for mixture velocity gives

$$\delta v_m(z,t) = \varepsilon e^{st} \Lambda_3(z,s) \tag{17}$$

where $\Lambda_2(z,s)$ and $\Lambda_3(z,s)$ are transfer functions. A detailed analysis and expressions for these transfer functions are given in ref. [12].

After solving for the kinematics of the fluid, the velocity field and the density variation are known, and the pressure drop can be calculated by integrating the momentum equation. By considering the heated section with the inlet and exit flow restrictions, the steady channel pressure drop becomes

$$\begin{aligned}
\Delta\bar{p}_{ext} = {} & k_i \rho_f \bar{v}_{fi}^2 + \rho_f \bar{v}_{fi}^2 \left[\frac{C_0 \bar{c}_k(l)}{(C_0 - 1)\bar{c}_k(l) + \bar{c}_k(\bar{\lambda})} - 1 \right] \\
& + \rho_f \left[g_0 l_i + g\bar{\lambda} + g \int_{\bar{\lambda}}^{l} \frac{(C_0 - 1)\bar{c}_k(z) + \bar{c}_k(\bar{\lambda})}{C_0 \bar{c}_k(z)} dz \right. \\
& \left. + \frac{g_e}{Cr^*} l_e \right] + \rho_f \bar{v}_{fi}^2 \left[\frac{f_0 l_i}{2D_0} \left(\frac{A_c}{A_0} \right)^2 + \frac{f_s \bar{\lambda}}{2D} \right. \\
& + \int_{\bar{\lambda}}^{l} \frac{f_m}{2D} \frac{C_0 \bar{c}_k(z)}{(C_0 - 1)\bar{c}_k(z) + \bar{c}_k(\bar{\lambda})} dz \\
& \left. + \frac{\bar{f}_{me}}{2D_e} \frac{C_0 \bar{c}_k(l)}{(C_0 - 1)\bar{c}_k(l) + \bar{c}_k(\bar{\lambda})} \left(\frac{A_c}{A_e} \right)^2 l_e \right] \\
& + \rho_g Cr^* (Cr^* - 1)[(C_0 - 1)^2 [\bar{v}_{fi} + \Omega(l - \bar{\lambda})]^2 \\
& + 2(C_0 - 1)[\bar{v}_{fi} + \Omega(l - \bar{\lambda})] v_{gj} + v_{gj}^2] \\
& + k_e \rho_f \bar{v}_{fi}^2 \frac{C_0 c_k(l)}{(C_0 - 1)\bar{c}_k(l) + \bar{c}_k(\bar{\lambda})}
\end{aligned} \tag{18}$$

where $Cr^* = \bar{c}_k(l)/\bar{c}_k(\bar{\lambda})$.

The first term is the inlet orifice term, the second is the convective acceleration term, the third (inside the square brackets) is the gravity term, the fourth (inside the square brackets) is the friction term, the fifth (inside the square brackets) is the drift stress term and the sixth is the exit orifice term.

A simplifying assumption is that $\rho_m - \rho_g = \rho_m$ in the drift pressure drop term. The two-phase friction factor

model used is $f_m = C_m f_s$. The value of the multiplier C_m depends upon inlet subcooling, inlet velocity, flow regime and system pressure [5]. For the conditions considered in the present work, $C_m = 1.5$ is a good approximation which gives pressure drops comparable with the Martinelli–Nelson correlation with a maximum error of about 18%.

Here, the first-order solution is given as a form of functional relationship between the perturbation of the system pressure drop and of the incoming fluid velocity:

$$\delta\Delta p_{ext}(s, t) = Q(s)\delta v(s, t) \tag{19}$$

where $Q(s)$ is the characteristic transfer function. According to control theory, the asymptotic stability of the system is determined from the nature of roots of the characteristic equation $Q(s) = 0$. For stability against flow excursion, it can be seen from equation (1) that the system will be stable against flow excursion if

$$\lim_{s\to 0} Q(s) = 0. \tag{20}$$

4. IMPORTANT SIMILARITY PARAMETERS

The characteristic equation is non-dimensionalized by choosing the length scale as the heated length, time scale as the reciprocal of the characteristic frequency of phase change, and the cross-sectional area of the heated section as the area scale. The basic parameters governing the system dynamics are the Froude number, Fr, the Reynolds number, Re, the subcooling number, N_{sub} the phase change number, N_{pch}, the drift number, N_d and the density number, N_ρ. The subcooling number takes into account the time lag effects in the heated liquid region due to the subcooling of liquid entering the heated duct. The phase change number scales the change of phase due to the heat transfer to the system. It decides the time lag in the heated mixture region. The drift number accounts for the diffusion effects due to the relative motion of fluids. It characterizes the flow pattern. The density number scales the system pressure.

The dimensionless characteristic equation can be expressed in terms of various similarity parameters as

$$Q^* = f(k_i, k_e, Fr, Re, N_{sub}, N_{pch}, N_d, N_\rho, s^*) = 0. \tag{21}$$

To present the stability boundaries in a two-dimensional plane, two representative parameters as the coordinates are required. For constant system pressure, inlet velocity, given fluid and geometry, the Froude number, the Reynolds number, the drift number and the density ratio are fixed. Hence, the subcooling and the phase change numbers are useful as the coordinates of the stability plane. The operational domain in the stability plane is bounded by the physical restriction on heat flux and subcooling. Figure 1(b) shows the stability plane with these basic characteristics.

Two computer codes are used for the numerical analysis. One is used to obtain the neutral stability curves and the other tests chosen points for stability. The parametric equations describing the neutral stability curve are obtained by separating the real and imaginary parts of the characteristic equation. The limiting value $\omega \to 0$ makes the imaginary part zero, thus the initial value of the real part decides the excursive stability boundary. The stability plane is bounded by the finite domain for its coordinates. A nodal mesh can be created by constant subcooling and quality lines. The crossover frequencies can be found by interpolation. These are substituted into the real part of the shifted characteristic equation and for non-zero values of the real part, the stability test is carried out. When the real part is zero, the point lies on the stability boundary. The stability boundaries are constructed by covering the entire mesh. The input data for the computer codes was obtained from Westinghouse Savannah River Company and Babcock and Wilcox Research and Development Center at Alliance, Ohio. The data consist of reactor geometry and operating conditions.

5. RESULTS AND DISCUSSION

5.1. *Density wave instability*

Figure 2 show the stability boundaries for flow excursions and density wave oscillations. Figure 2(a) also shows higher order solutions; but when the system crosses the first stability boundary, it goes into oscillations that are likely to damage the system, hence the first stability boundary is the most important one. Higher order solutions are not important. Figure 2(c) shows both the excursion and density wave boundary. It is important to note that flow excursions are important for low subcooling, whereas density wave oscillations are predominant for high subcooling.

Figures 3–6 describe the effects of various operational parameters on the stability of the system. It is important to note that density wave oscillations and excursion occur at low exit qualities. Figure 3 describes the effect of inlet velocity (represented by the Reynolds number) on the stability of the system. An increase in the inlet velocity reduces the effects of both the gravitational force and the relative velocity. The kinematic effects of change inthe inlet velocity are largely reflected in the ordinate itself. Since the friction factor is not a very strong function of the Reynolds number for turbulent flow, if the inertial, frictional and orifice pressure drops dominate the fluid dynamics, then the change in inlet velocity is reflected significantly in the phase change number. All the curves in Fig. 3 almost overlap, and hence it can be concluded that the effects of velocity are taken into account by the phase change number.

Figures 4 and 5 describe the effect of inlet and exit throttling on the stability of the system. Increased

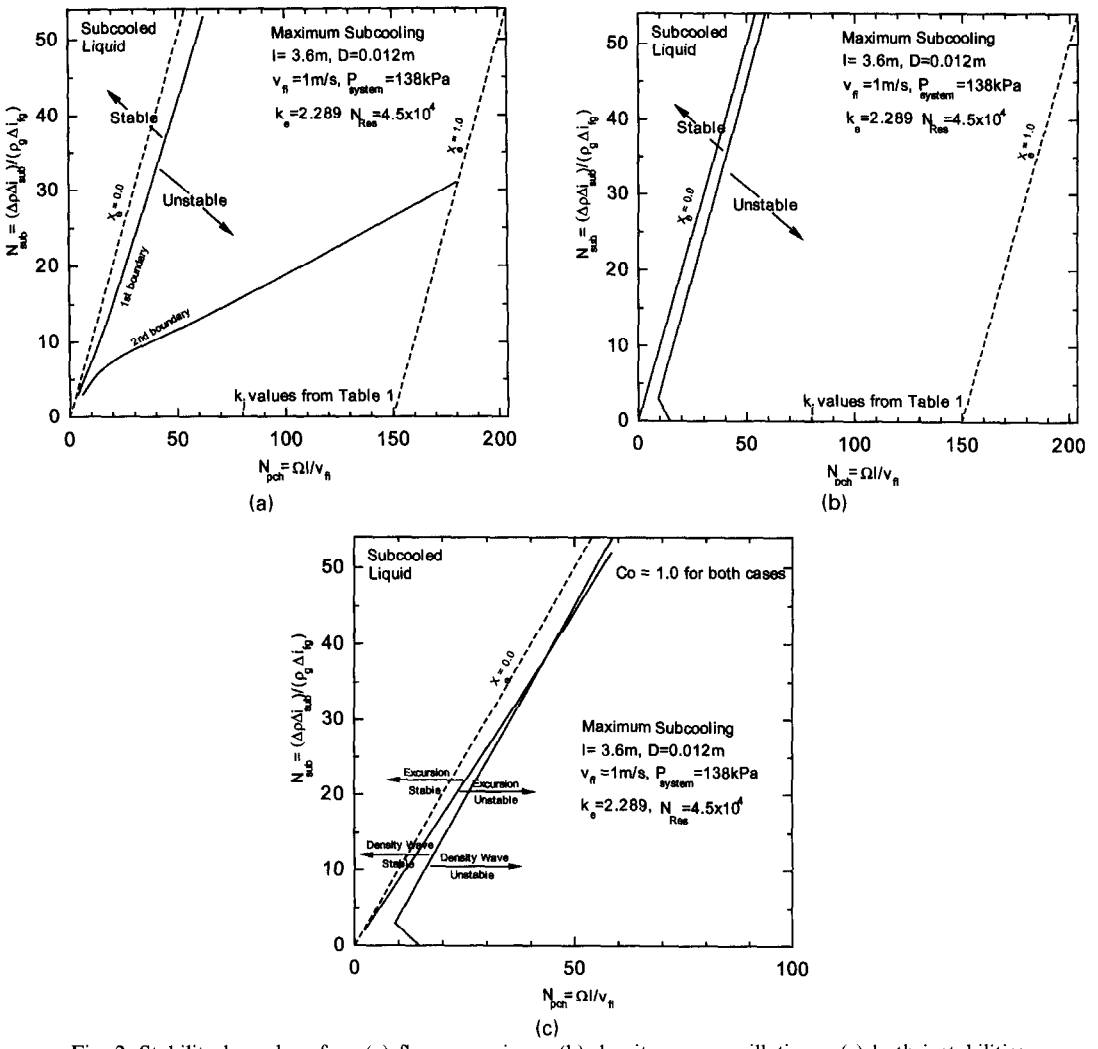

Fig. 2. Stability boundary for: (a) flow excursions; (b) density wave oscillations; (c) both instabilities together.

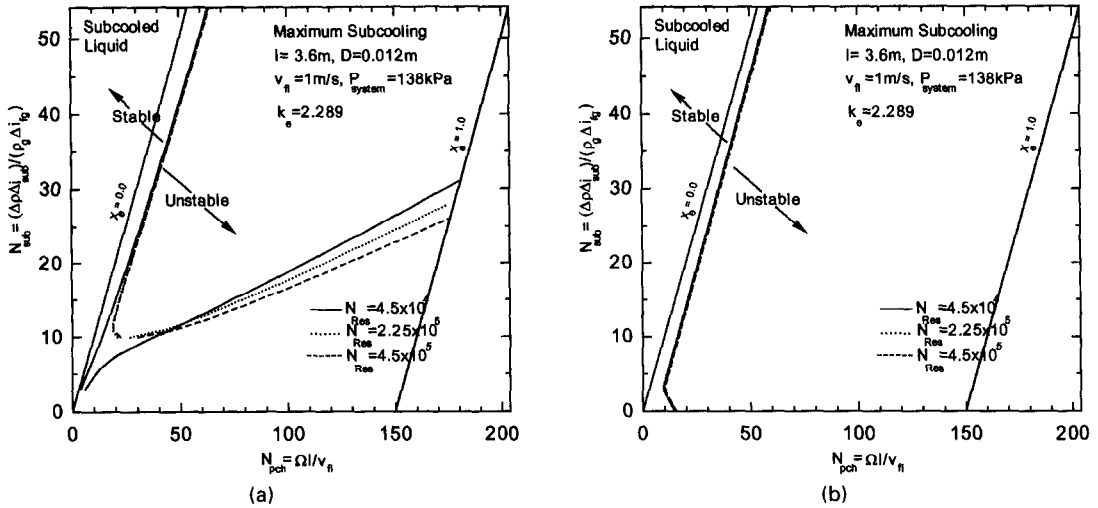

Fig. 3. Effect of inlet velocity on the stability boundary for: (a) flow excursions; (b) density wave oscillations.

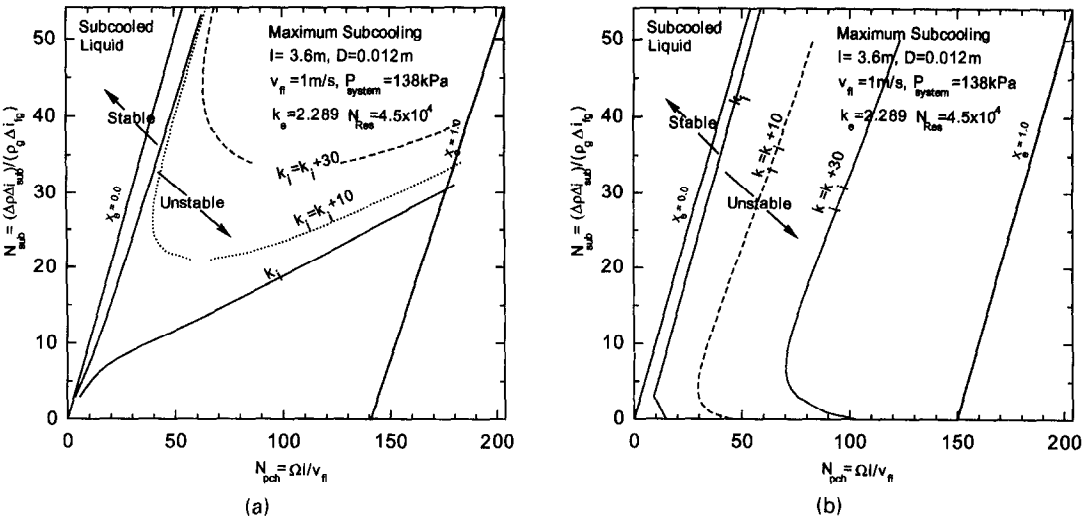

Fig. 4. Effect of inlet throttling on the stability boundary for: (a) flow excursions; (b) density wave oscillations.

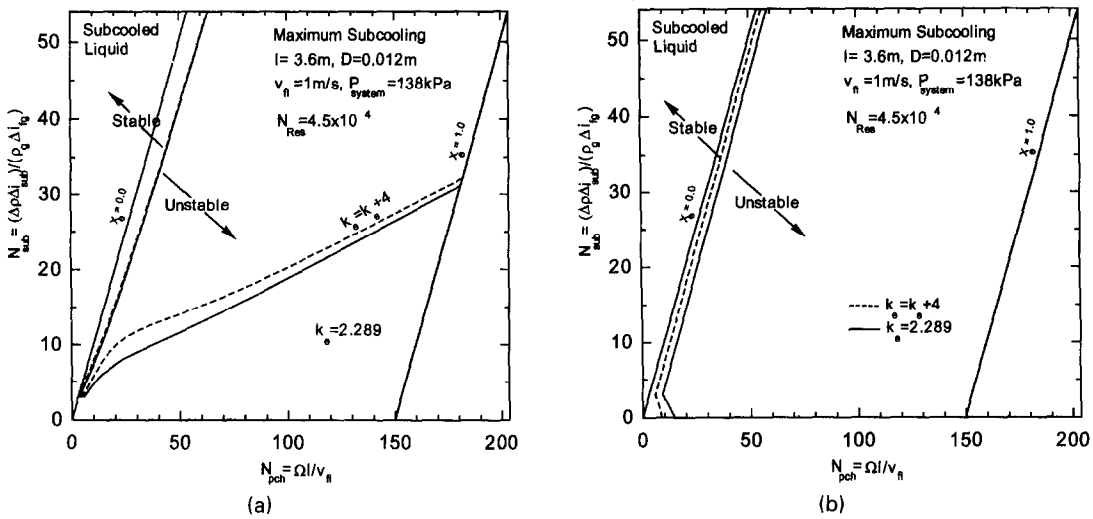

Fig. 5. Effect of exit throttling on the stability boundary for: (a) flow excursions; (b) density wave oscillations.

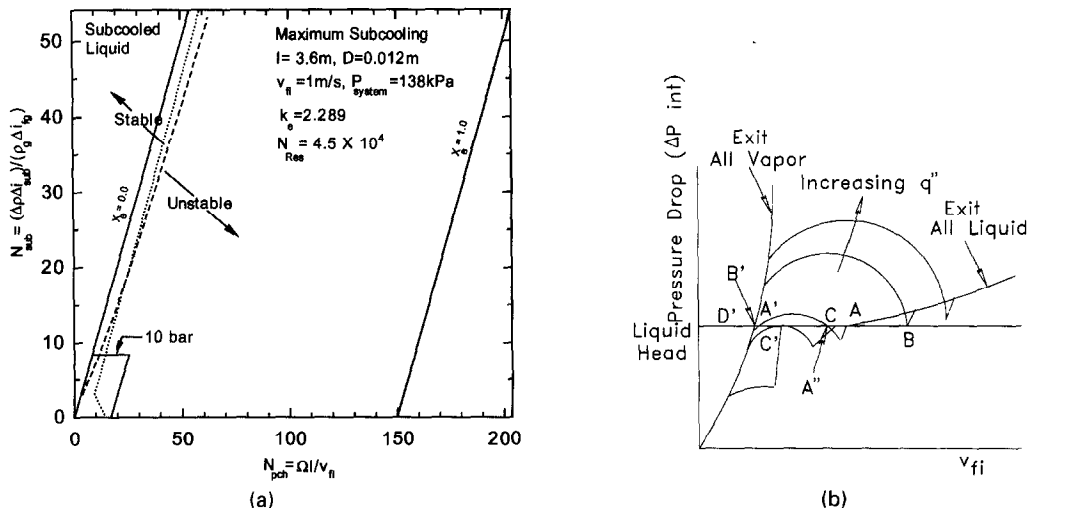

Fig. 6. (a) Effect of system pressure on system stability; (b) internal pressure drop as a function of inlet flow.

inlet throttling tends to stabilize the system, whereas increased exit throttling tends to destabilize the system. This is because the inlet pressure drop is in phase with the inlet velocity. The exit pressure drop is in phase with the mixture velocity, but the mixture velocity is not in phase with the inlet velocity due to the time lag in wave propagation.

Figure 6(a) describes the effect of system pressure on the stability of the system. The system pressure mainly affects the exit quality, and hence in terms of the exit quality, the system pressure significantly stabilizes the flow. However, in terms of the phase change number, there are no appreciable effects of the system pressure. For very small subcooling, the stability boundary curve itself has a large change in the phase number compared with the subcooling number. Hence, the numerical data points are difficult to obtain accurately. Also, for low subcooling, the effect of subcooled boiling may have a significant influence on the system stability. Subcooled boiling may dominate the entire heated region. In that case, phase change proceeds further than in the case of thermal equilibrium and the value of phase change number increases.

5.2. *Flow excursion and critical heat flux*

By equating the internal pressure drop to the external driving head, the inlet flow can be calculated as a function of the heat flux. A sample calculation is performed and is illustrated with the help of Fig. 6(b). Figure 6(b) shows the internal pressure drop as a function of inlet flow for various values of heat flux while the subcooling is held constant. The horizontal line represents the external driving head. Two limiting cases of all vapor and all liquid conditions at the exit are also shown. The S-curves connecting these two limits are the internal pressure drop vs inlet flow curves calculated from the steady pressure drop expressions for regions [A]–[D]. The intersection of these curves with the available pressure drop (horizontal line) represent possible operating conditions. The operation is stable if the intersection occurs in that portion of the S-curve that has a positive slope [10]. It follows that all operational points with a negative slope are exclusively unstable and therefore cannot be sustained under steady state conditions.

Figure 7 shows all the possible solutions in terms of inlet velocity and heat flux. For certain values of heat flux, the solution for inlet velocity is multivalued. Hence, for these conditions the operational conditions depend on past history. The region from C′ to C is the most important for reactor safety. It shows whether the reactor can be recovered from the high quality mode. A parametric study for external driving head reveals that when the external driving head drops below 1.2 times the value of the hydrostatic head, the system cannot be recovered from the high quality mode, even by reducing the heat flux to zero. Enthalpy burnout is certain if the heat flux is not reduced to a value less that 5% of the full power. Figure 7 also indicates the exit quality values at excursion points. The possibility of system recovery can be judged by these values.

5.3. *Flooding and flow regime transition*

Flooding and churn-turbulent to annular flow regime transition are two important static instabilities that can result in the occurrence of critical heat flux at low flow [8]. Hence, it is worthwhile to predict these instabilities for given operating conditions. Critical heat flux due to flooding occurs when the bottom of the subassembly is blocked. The net flow through the system is zero because the vapor prevents any downward flow of liquid. The flooding correlation expressed in terms of heat flux [7] is

$$q'' = \frac{A}{A_h}\left(\frac{1}{C_0} - 0.11\right)\Delta i_{fg}\sqrt{(\rho_g \Delta\rho g D)} \qquad (22)$$

where A is the flow area and A_h is the heated area. In terms of stability plane parameters,

$$(N_{pch})_c = \left(\frac{1}{C_0} - 0.11\right)\frac{\Delta\rho}{\rho_g \rho_f \bar{v}_{fi}}\sqrt{(\rho_g \Delta\rho g D)}. \qquad (23)$$

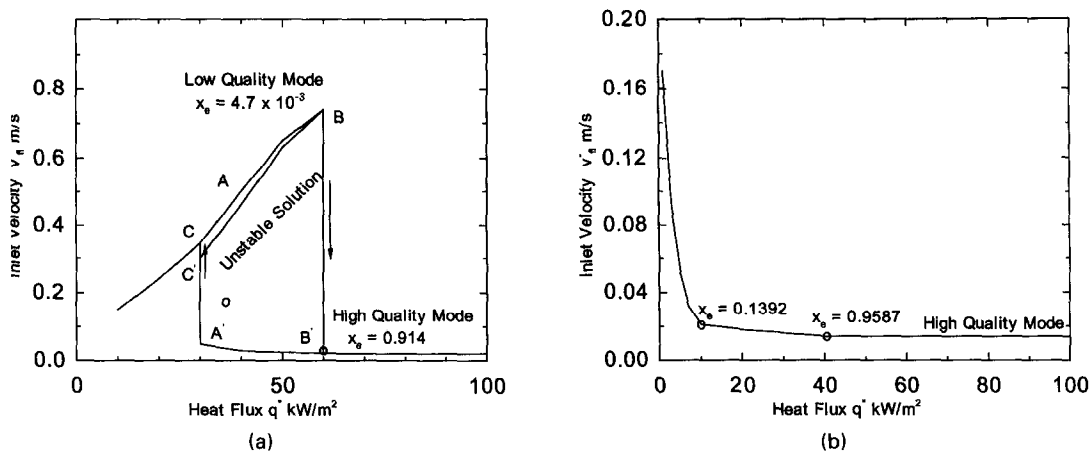

Fig. 7. Inlet flow as a function of heat flux: (a) $\Delta p_{ext} = 1.2 \times$ hydrostatic head; (b) $\Delta p_{ext} = 1.1 \times$ hydrostatic head.

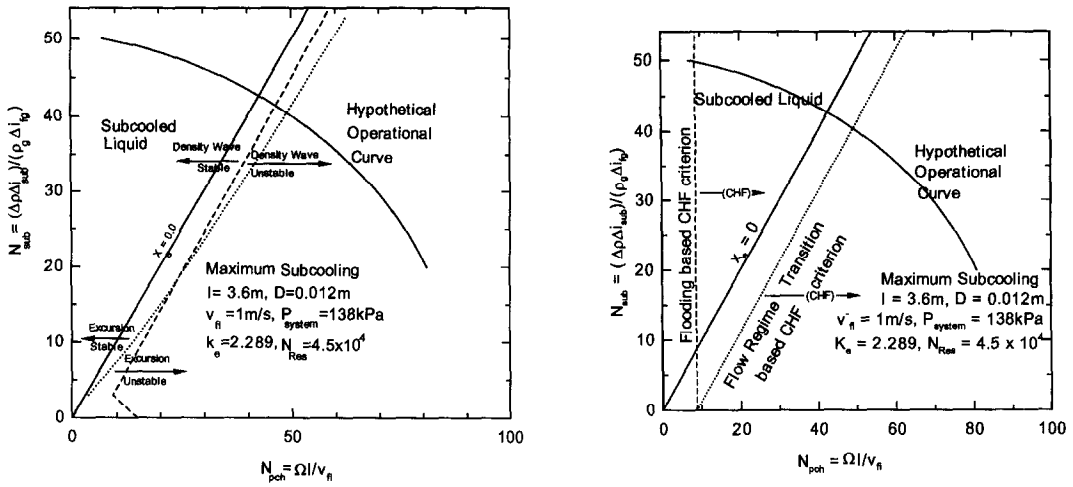

Fig. 8. Hypothetical operation curve with: (a) flow excursion stability boundary and density wave oscillation boundary; (b) churn-turbulent to annular flow regime transition-based critical heat flux criterion and flooding-based critical heat flux criterion.

Critical heat flux due to the flow regime transition from churn-turbulent to annular flow occurs at low flow and low pressure conditions [8], due to the dryout of the film which cannot be wetted by the liquid slug. The churn-turbulent to annular flow regime transition, expressed in terms of heat flux [7], is

$$q'' = \frac{A}{A_h}\left[\Delta i_{sub}\rho_f \bar{v}_{fi} + \left(\frac{1}{C_0} - 0.11\right)\Delta i_{fg}\sqrt{\rho_g \Delta\rho_g D}\right]. \tag{24}$$

In terms of stability plane parameters:

$$(N_{pch})_c = N_{sub} + \left(\frac{1}{C_0} - 0.11\right)\frac{\Delta\rho}{\rho_g\rho_f \bar{v}_{fi}}\sqrt{\rho_g \Delta\rho_g D}. \tag{25}$$

Consider a hypothetical operation curve for the reactor. Figure 8 shows the plots of the operation curve in the stability plane along with flow excursions, density wave oscillations, flooding criterion and churn-turbulent flow regime transition, respectively. The results give a quantitative basis to predict which instability is encountered first under the given operating conditions. Since the operation curve is hypothetical, the results are not exact; but the important point is that if a correct operation curve is available, the analysis will predict the behavior of the system.

5.4. *Comparison with flow excursion experimental data*

A description of the transient events and phenomena and a complete set of test data plots associated with the most severe test LOCA are reported in ref. [14] for Test 867-12. The data for flow as a function of power are compared with the results of calculations performed using the present analysis, and the results are shown in Fig. 9.

The transient passes through three regions, namely excursion, high quality mode and recovery. Comparing Fig. 9 with Fig. 7(a) or Fig. 7(b), the transient is seen to follow the path from B to B′ (excursion), B′ to A′ (high quality mode) and A′ to C (recovery). It is seen from the figure that the two sets of values are in fair agreement, with a maximum error of about 20%, and hence the result is satisfactory. Two possible reasons that can be given for the difference are: the subcooling used for LOCA tests is very high compared with the values used for the present analysis—this shows that subcooled boiling is very important in LOCA tests, and the assumption of thermal equilibrium (used in the present analysis) may not hold; next, the axial power profile for LOCA tests is not uniform (another assumption in the present analysis), but simulates the profile for the reactor. This would affect the onset of instabilities.

6. SUMMARY AND CONCLUSIONS

For a low pressure system with downflow typical of heavy water isotope production reactors and other

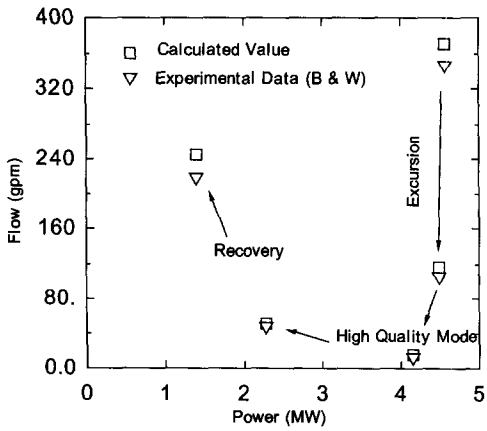

Fig. 9. Comparison of Babcock and Wilcox experimental data with present predicted values.

research reactors, the occurrence of the critical heat flux under a loss-of-flow or loss-of-coolant accident is significantly affected by various flow instabilities and hydrodynamic transitions. A detailed stability analysis for downflow systems has been carried out by using the one-dimensional drift flux model and small perturbation method. The stability boundary for the flow excursion as well as for the density wave instability have been obtained from the D-partition method. The results are presented in the stability plane. Other important hydrodynamic transitions which can trigger the critical heat flux phenomena are also studied. A general approach for studying the occurrence of these instabilities and transitions relative to the system operational transient condition can be plotted on the stability plane, thus one can identify the occurrence of these instabilities and the time sequences by the intersection of the stability boundary curves and the system transient curve. This approach gives a simple and practical method for studying the effect of these various instabilities.

Acknowledgements—This research was supported by Westinghouse Savannah River Site (SRS) through the Department of Energy, Office of Energy Research, Nuclear Engineering Research Grant Program. The authors would like to express their sincere appreciation to Drs C. Apperson and J. Steimke of SRS and Drs D. Woodall and T. J. Dolan of INEL and the staff of DOE and SRS. The authors would also express their sincere appreciation to Dr U. S. Rohatgi for his comments.

REFERENCES

1. J. L. Achard, D. A. Drew and R. T. Lahey Jr, The analysis of non-linear density wave oscillations in boiling channels, *J. Fluid Mech.* **155,** 213–232 (1985).
2. A. E. Bergles, Instabilities in two-phase systems. In *Two-phase Flow and Heat Transfer in Power Process Industries* (Edited by A. E. Bergles, T. G. Collier, J. M. Delhaye, G. F. Hewitt and F. M. Mayinger), pp. 383–423. Hemisphere, Washington, DC (1981).
3. J. Boure', The oscillatory behaviour of heated channels, Technical Report C.E.A.R. 3049, Centre d'Etudes Nucleaires de Grenoble, France (1966).
4. J. Boure', A. E. Bergles and L. S. Tong, Review of two-phase flow instability, *Nucl. Engng Design* **25,** 165–192 (1973).
5. M. Ishii, Thermally induced flow instabilities in two-phase mixtures in thermal equilibrium, Ph.D. Thesis, Georgia Institute of Technology, GA (1971).
6. M. Ishii and N. Zuber, Thermally induced flow instabilities in two-phase mixtures, *Proceedings of the Fourth International Heat Transfer Conference*, Vol. 5, Paper No. 5.11. Paris (1970).
7. K. Mishima, Boiling burnout at low flow rate and low pressure conditions, Ph.D. Thesis, Research Reactor Institute, Kyoto, Japan (1984).
8. S. J. Peng, M. Z. Podowski and R. T. Lahey Jr, Digital computer code for linear stability analysis of boiling water nuclear reactors, Technical Report NUREG/CR 4116, Nuclear Regulatory Commission (1985).
9. R. P. Taleyarkhan, A. F. McFarlane, M. Z. Podowski and R. T. Lahey Jr, Impact of transient single phase heat transfer modeling on predicted BWR fuel stability margin, *Trans. Am. Nucl. Soc.* **55,** 747 (1987).
10. G. B. Wallis and J. H. Heasley, Oscillations in two-phase flow systems, *J. Heat Transfer* **83c,** 363–369 (1961).
11. N. Zuber, Flow excursions and oscillations in boiling two-phase flow systems with heat addition, *Proceeding of the Symposium on Two-phase Flow Dynamics*, EUR4288e, Vol. II, pp. 1071–1109. CEC, Eindhoven (1967).
12. S. Lele, Stability analysis of two-phase downflow and its effect on critical heat flux phenomena, M.S. Thesis, Purdue University (1992).
13. M. Ledinegg, Instability of flow during natural and forced circulation, *Die Warme* (Translation in USAEC-tr-1861) **61,** 891–989 (1932).
14. G. C. Rush, J. E. Blake and C. A. Nash, Flow excursion experiments with a Savannah River Mark 22 fuel assembly mockup, Technical Report RDD: 90: 4427-13-01-01: 01, Babcock and Wilcox R and D Division (1990).